BL-8A/2010G501, BL-7C/2010G502,

Structural and electronic properties of Mn hexacyanoferrates against Li

Tomiyuka Matsuda, Yutaro Kurihara[1] and Yutaka Moritomo[1,2]
[1]Graduate School of Pure and Applied Science, University of Tsukuba, Tsukuba 305-8571, Japan
[2]Tsukuba Research Center for Interdisciplinary Materials Science (TIMS), University of Tsukuba, Tsukuba305-8571, Japan

1 Introduction

Recently, Okubo *et al.*[1] reported the reversible Li ion intercalation properties in $K_{0.14}Mn_{1.43}[Fe(CN)_6]\cdot 6H_2O$ and $Rb_{0.7}Mn_{1.15}[Fe(CN)_6]\cdot 2.5H2O$. We have also demonstrated that a thin film of $Li_{1.32}Mn[Fe(CN)_6]_{0.83}\cdot 3.5H_2O$ shows a large charge capacity (= 128 mAh/g) as well as excellent cyclability,[2] which indicates that the Prussian blue analogues are one of the promising cathode materials for the Li ion secondary batteries. In this Li ion intercalation process, Mn^{II}/Mn^{III} reduction/oxidation occurs and the cooperative Jahn-Teller instability can be expected. In this work, we prepared two $Li_xMn[Fe(CN)_6]_y\cdot zH_2O$, which have different amount of $[Fe(CN)_6]$ vacancy sites and investigated the electronic states and structural properties.

2 Experiment

Thin films of $Na_{1.32}Mn[Fe(CN)6]_{0.83}\cdot 3.5H_2O$ were electrochemically synthesized on an indium tin oxide (ITO) transparent electrode under potentiostatic conditions at −0.50 V vs a standard Ag/AgCl electrode in an aqueous solution containing $K_3[Fe(CN)_6]$ (1.0 mmol dm−3), $MnCl_2\cdot 6H_2O$ (1.5 mmol dm^{-3}), and NaCl (1 mol dm^{-3}). Before the film growth, the surface of the ITO electrode was purified by electrolysis of water for 3–5 min. The obtained film was transparent with a thickness of around 1 μm. Chemical compositions of the films were determined by the inductively coupled plasma (ICP) method and CHN organic elementary analysis (Perkin-Elmer 2400 CHN Elemental Analyzer). The Na ions were electrochemically substituted by Li ions, using lithium metal as the reference and counter electrode, and ethylene carbonate (EC) / diethyl carbonate (DEC) solution containing LiClO4 (1 mol dm^{-1}) as an electrolyte. Thus, we obtained $Li_xMn[Fe(CN)6]_{0.83}\cdot 3.5H_2O$ (LMF83).

The electronic states of the Mn and Fe sites of LMF83 against x were determined by the *ex-situ* X-ray absorption spectra (XAS) around the Mn and Fe K-edge. The XAS measurements were conducted at the beamline 7C of the Photon Factory, KEK. The XAS spectra were recorded by a Lytle detector in a fluorescent yield mode with a Si(111) double-crystal monochromator at 300 K. The background subtraction and normalization were conducted by ATHENA program [3].

The *ex-situ* powder X-ray diffraction (XRD) measurements of L*x*MF83, and LMF87 against x were performed at the beamline 8A of KEK-PF, equipped with an imaging plate detector. The samples were washed with DEC, and carefully removed from the ITO glasses. The obtained powders were sealed in 300 μm glass capillaries. XRD patterns were measured at 300 K and the exposure time was 5 min. Wavelength of the X-ray was 0.77516 Å. The lattice constants of each compounds were refined by the RIETAN-FP program [4].

3 Results and Discussion

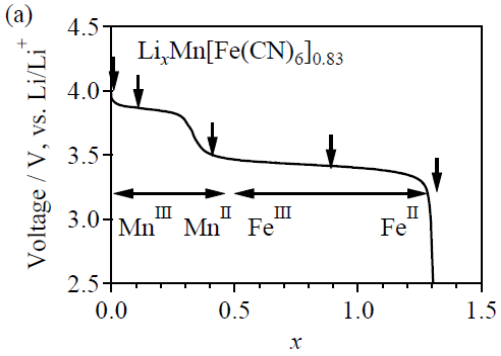

Figure 1. Voltage dependence on Li ion concentration (x) of L*x*MF83. The arrows indicate x for the XAS measurements

Figure 1 shows the voltage against Li metal dependence on x of LMF83 during the Li ion intercalation process. Here, the possible x regions are $0 \le x \le 1.32$ for LMF83 due to the charge neutrality. On both films, the electrochemical reactions were observed at around 3.8, and 3.4 V.

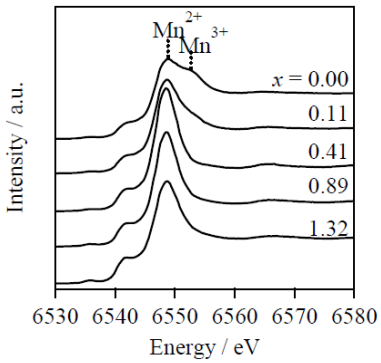

Figure 2. Mn K-edge XAS spectra of LMF83.

Figure 2 shows the Mn K-edge XAS spectra of L*x*MF83 against x. The peak around 6549 eV, which is ascribed to Mn^{II}, was observed in the whole-x region. On the contrary, the shoulder peak around 6552 eV, which is ascribed to Mn^{III}, was observed in the small-x region. These spectra indicates the reduction/oxidization of Mn (high-spin Mn^{II}, and high-spin Mn^{III}) occurs in the small-x region. Figure 3

shows the Fe K-edge XAS spectra of L*x*MF83 against *x*. The absorption peak energies (*E*) in the Fe K-edge spectra show clear blue shift with decrease in *x*, and saturate below $x = 0.41$. These data indicates blue shift is ascribed to the oxidization of Fe (low-spin $Fe^{II} \rightarrow$ low-spin Fe^{III}), and indicates the reduction/oxidization of Fe takes place in the large-*x* region. Considering the formula and the range of *x*, the reduction/oxidization of Fe occurs in $0.49 \leq x \leq 1.32$ region, while the reduction/oxidation of Mn occurs in $0 \leq x \leq 0.49$ region in LMF83. Hence, the first plateau in Figure 1 corresponds to the Mn^{3+}/Mn^{2+} reduction process, and the second plateau in Figure 1 corresponds to $[Fe^{III}(CN)_6]^{3-}/[Fe^{II}(CN)_6]^{4-}$ reduction process.

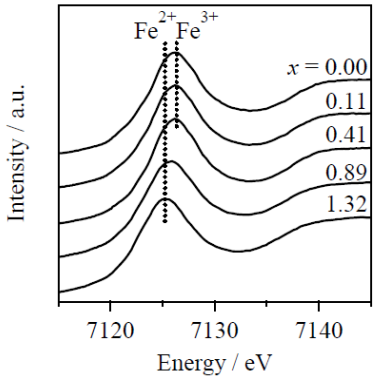

Figure 3. Fe K-edge XAS spectra of LMF83.

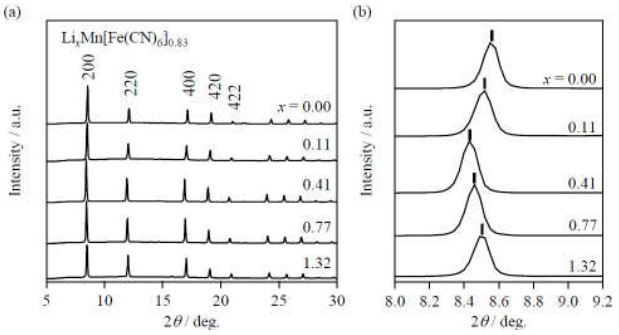

Figure 4. (a) The powder XRD patterns for LMF83. (b) Magnified patterns around the 200 reflection. The ticks indicate the reflection peak positions. The wavelength of the X-ray is 0.77516 Å.

Figure 4(a) shows the XRD patterns of LMF83. The peak patterns are all similar, which indicates that the lattice structure remains the face-centered cubic ($Fm\underline{3}m$; $Z = 4$) throughout whole *x* region. Figure 4(b) shows the magnified patterns around the 200 reflection. The reflection shifts to the lower-angle side with *x* above $x = 0.41$, while it shifts to the higher-angle side with *x* above $x = 0.41$. The value of $x = 0.41$ is close to the value of $x = 0.49$ where reduction/oxidation switch between Mn and Fe occurs. In the reduction/oxidation of Fe region ($0.49 \leq x \leq 1.32$), the lattice constants decreases with *x*. The decrease is ascribed to the smaller size of $[Fe^{II}(CN)_6]^{4-}$ as compared with that of $[Fe^{III}(CN)_6]^{3-}$. In the reduction/oxidation of Mn region ($0 \leq x \leq 0.49$), the lattice constants increase with *x*. The increase is ascribed to the larger ionic radius of high-spin Mn^{II} (0.83 Å) than high-spin Mn^{III} (0.645 Å).

Acknowledgement (option)
This work was supported by a Grant-in-Aid (21244052) for Scientific Research from the Ministry of Education, Culture, Sports, Science and Technology. Elementary analysis was performed at Chemical Analysis Division, Research Facility Center for Science and Engineering, University of Tsukuba.

References

[1] M. Okubo, *et al*., *J. Phys. Chem. Lett.* **1**, 2063 (2010).
[2] T. Matsuda and Y. Moritomo, *Appl. Phys. Express* **4**, 047101 (2011).
[3] B. Ravel and M. Newville, *J. Synchrotron Radiat*. **12**, 537 (2005)
[4] F. Izumi and K. Momma, *Solid State Phenom.* **130**, 15 (2007).

* moritomo.yutaka.gf@u.tsukuba.ac.jp